CHAPTER 7

A. Pressure induced semimetal to metal transition in $MoTe_{2-x}Se_x$ and $WTe_{2-x}Se_x$

7.A.1 Introduction

Transition-metal dichalgogenides (TMDCs) have taken immense research interest in recent times due to their various exotic properties like optoelectronics [342], [343], spintronics [344], [345], nanoelectronics [346], [347] and valleytronics [348]. These TMDCs have 2D layer crystal structure with a chemical formula MX_2 where M=Mo,W; X=Te,Se,S. The common structure of $MoTe_2$ is semiconducting 2H-phase(hexagonal), while the WTe_2 is normally formed in T_d-phase. The centrosymmetric 1T′(monoclinic)structure possesses the P21/m space group, whereas the T_d phase(orthorhombic) belongs to the non-centrosymmetric space group Pmn21 for $MoTe_2$. Both are semimetallic in nature. Weyl fermions occur in the T_d phase when the inversion symmetry is broken; T_d-$MoTe_2$ and WTe_2 are considered to be type-II Weyl semimetal [55], [349], [350]. On the other side, $MoSe_2$ and WSe_2 have controllable bandgaps that change from indirect to direct in monolayers [351], [352], allowing them for various emerging technological applications. The indirect to direct gap transition of monolayer MX_2 shows enhanced photoluminescence (PL) [353], [354]. $WTe_{2-x}Se_x$ exhibit in semiconducting 2H and metallic T_d phase [355].

Pressure is a unique tool to probe the changes in electronic structure of the TMDCs and topological materials like $MoTe_2$ [356] and WTe_2 [357], $Mo_{1-x}W_xTe_2$ [358] and MoSSe [359]. Various electronic changes such as semiconductor to metal transition and structural transitions like T_d to 2H/ 1T′/T_d*are possible under pressure. Based on the above idea present study also explore the electronic properties of $MoTe_{2-x}Se_x$ and $WTe_{2-x}Se_x$ (x=1) under the extreme conditions and compare the results with ambient one.

The present work reveals that MoTeSe and WTeSe both are semimetallic system with equal hole and electron contributions, also there is a Dirac like dispersion for WTeSe without the crossing between band extrema.

7.A.2 Methods

First-principles calculations were performed with VASP (Vienna *ab initio* simulation package) using Perdew-Burke-Ernzerhof (PAW) potential with generalized gradient approximation (GGA). A plane wave cutoff energy of 500eV adopted for the calculations. A 15×9×5 K-mesh is used for the self-consistent field (SCF) run. All the atom positions are fully relaxed through the conjugate-gradient algorithm until the residual force less than 0.01 eV A^{-1}. Optimized lattice parameters of MoTeSe are a= 3.387, b= 6.163, c= 13.905 Å and WTeSe are a= 3.405, b= 6.091 and c=14.804 Å.

7.A.3 Result and Discussion

The band structure of MoTeSe and WTeSe are very similar to each other as they both belong to same family. In Figure 7.A.1 (a) and (b), the band structure of both the compounds with spin orbit coupling (SOC) is represented. The bands get splitted with inclusion of SOC. Both MoTeSe and WTeSe has semimetallic character as the PDOS and total DOS showing vanishing DOS at the Fermi level as shown in Figure 7.A.2 (a, b) and insets. Moreover, the electronic characteristics of both are similar to semimetallic Weyl semimetal candidate $MoTe_2$ [181]. Although, the conduction band crossing the Fermi level at 0 pressure in the WTeSe we found $MoTe_2$-like DOS character in this material. The electronic states of both the compounds are mainly dominated by Mo-4d and W-5d orbitals. The VBM and CBM have also contributions from 5p orbital of Te and 4p orbitals of Se. The results demonstrate band-gap narrowing and metallization features under pressure. A Dirac-like dispersion features can be viewed between Z and U high symmetry points in WTeSe but there are no band crossings as evident from figure1 (b).

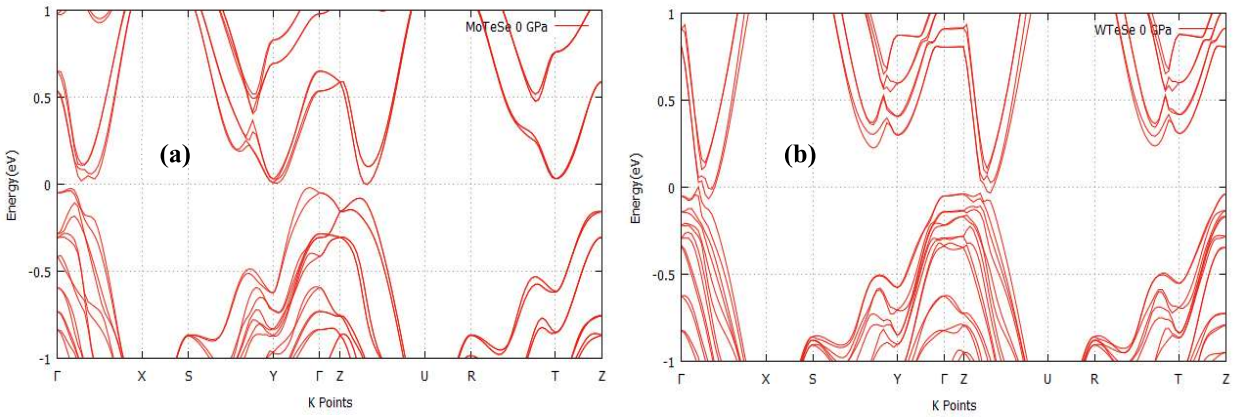

Figure 7.A.1 (a) Theoretical band structure of MoTeSe and (b) WTeSe with SOC at ambient conditions.

As the Mo/W and Te, Se having high atomic Z so the SOC splitting is quite large in these compounds are large. The metallization occurs at 3 GPa for Mo-based compound. A finite DOS at the Fermi level is clear from Figure 7.A.3 (a). With further increase in pressure metallic character increases Figure 7.A.3 (b). The CBM and VBM crosses the Fermi level significantly at this pressure. Similar to other TMDs MX_2, the shifts of CB valley minima and VB valley maxima driven by pressure produce a number of electron pockets and hole pockets. Figure 4 (a) and (c) displays the theoretical bandstructure of MoTeSe at 3 GPa and 10 GPa and their respective DOS are shown in Figure 7.A.3 (a) and (b). An indirect band gap at Y and T point is noticeable. The band gap decreases at those points with increase in pressure. At 3 GPa, the CBM valley at T and Y point crosses the Fermi level, this is the pressure where metallic character begins. The band structure consists of a direct bandgap along Γ-X and Z-U symmetry line. At high pressure the direct band gap feature is destroyed Figure 7.A.4 (c). The valence band gets flatter along Z-U symmetry path with increasing pressure. The DOS [Figure 7.A.2(a)] of MoTeSe possess an indirect band gap 0.049 eV, the VBM is -0.015eV and CBM is +0.034eV with respect to the Fermi level.

Our theoretical calculation illustrates that at the atmospheric conditions the semimetallic MoTeSe and WTeSe are perfect electron hole compensated system which could be

described by two band model similar to many other topological semimetallic systems [157], [181], [360], [361]. In 2H-$MoTe_2$, a semiconducting to metallic transition occurred at 10 GPa due to increased interlayer interaction coupling [362]. Again the 2H-$MoSe_2$ undergoes the same phase transition at 58 GPa from theoretical prediction [205].

In table 7.A.1, a comparative study of electronic and structural transition in MX_2 class of materials are given.

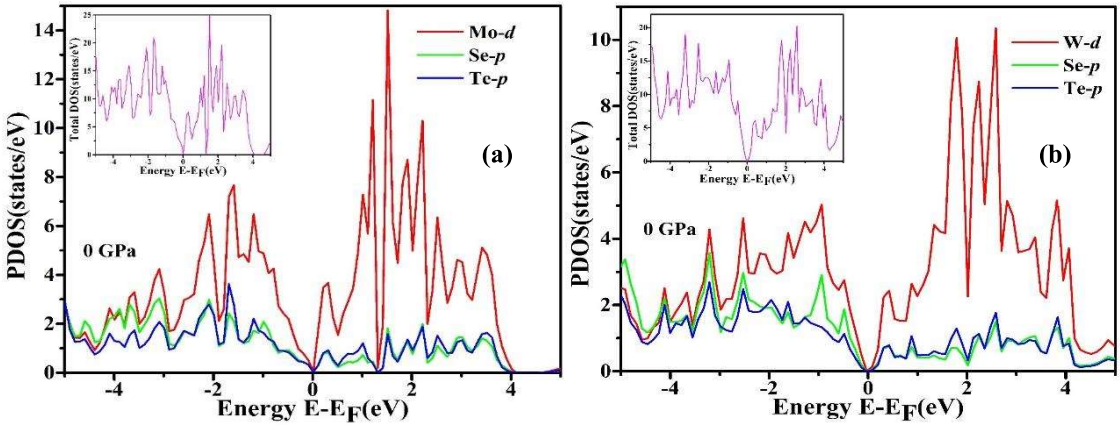

Figure 7.A.2 (a) Partial density of states (PDOS) of MoTeSe and (b) WTeSe at ambient pressure; inset: Total density of states (TDOS).

Table 7.A.1 Electronic and structural transitions under pressure.

Material	**Type of transition**	**Pressure (GPa)**
$MoTe_2$ [356]	metallization	13
WTe_2 [363]	Td→2H phase	10
MoSSe [359]	electronic	3
$MoTe_2$ [364]	Td→T_d^* phase	0.15
WTe_2 [357]	Td→1T′	6
WSe_2 [365]	metallization	35
$MoSe_2$ [366]	metallization	26.1

In Figure 7.A.5 (a) and (c) the evolution of lattice parameters a, b, c with pressure are shown for the two materials. In inset their respective c/a as a function of pressure is plotted. The compression in lattice parameters with increasing pressure is relatively larger along c direction for both the compounds. This is due to weaker van der Waals interlayer forces than stronger intralayer covalent bonding. The c/a ratio is 4.11 at ambient pressure and decreases to 3.79 at 10 GPa for MoTeSe. This parameter is 4.35 at 0 pressure and decrease to 3.84 at 10 GPa for the compound WTeSe.

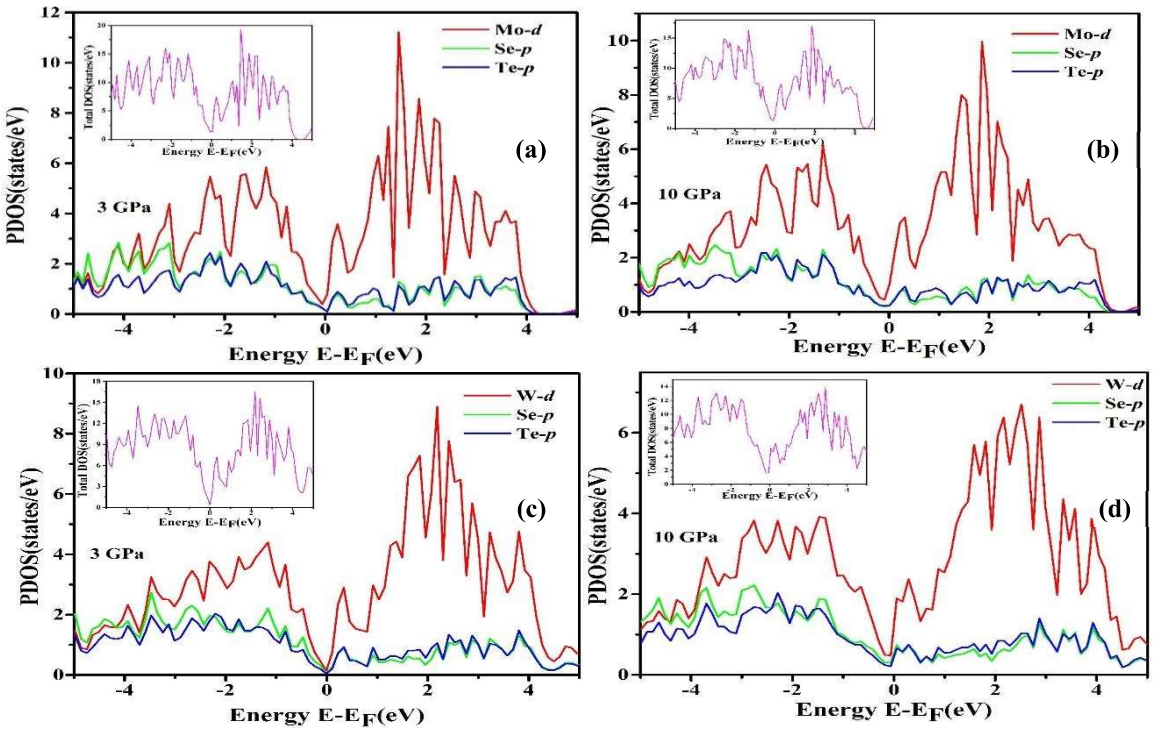

Figure 7.A.3 (a) PDOS and total DOS (inset) of MoTeSe at 3 GPa and (b) 10 GPa; (c) PDOS and total DOS (inset) of WTeSe at 3 GPa and (d) 10 GPa.

Previous reports on semiconducting $2H_c$-WSe_2 resistivity measurement reveals pressure induced semiconducting to metal transition at 1.8K in the pressure range 28.2-61.7GPa [367]. The same transition was observed in WSe_2 at 35 GPa by theoretical prediction [365]. This transition raised due to covalent character of W-Se bonding. Although a structural transition of T_d to 1T′ was displayed in [357] however no metallic transition was reported

in this phase. Our observation on the semimetallic phase of WTeSe shows metallic transition under pressure. The metallicity further increases with pressure.

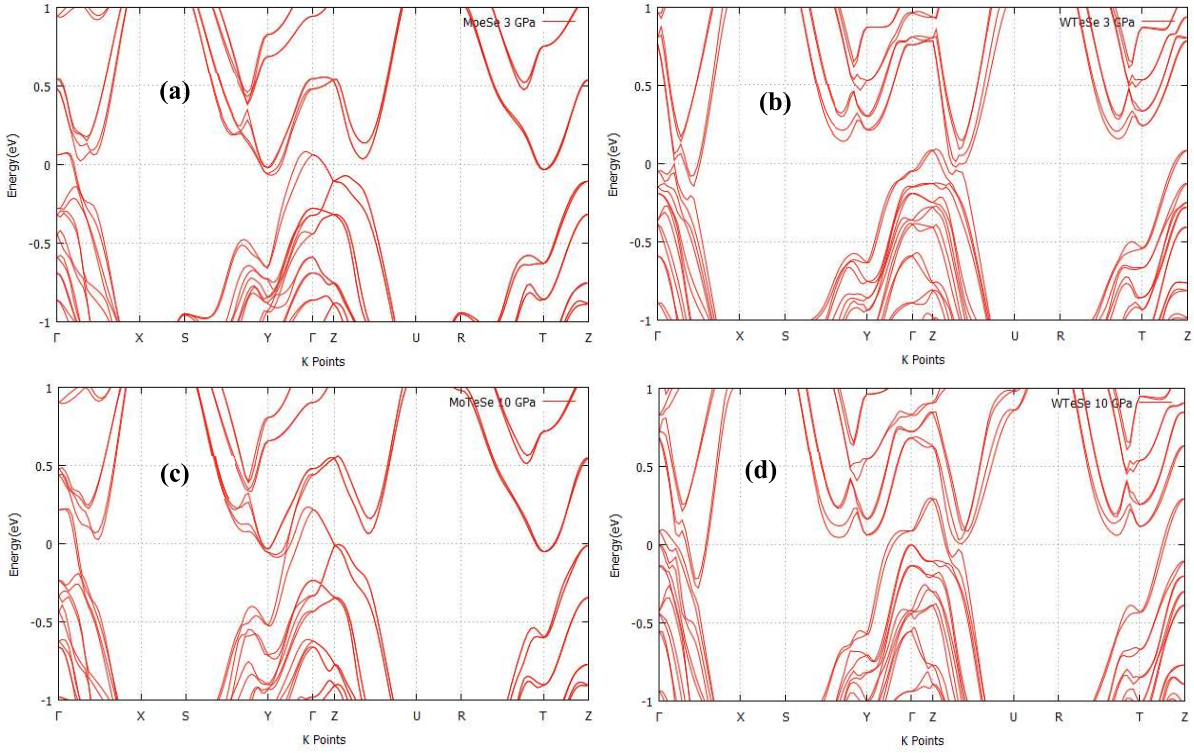

Figure 7.A.4 (a) Theoretically obtained band structure of MoTeSe at 3 GPa and (c) 10 GPa; (b) WTeSe at 3 GPa and (d) 10 GPa.

This result is consistent with [362]. The bandstructures at 3 GPa and 10GPa are shown in figure 4 (b) and (d) and their respective DOS are presented in figure 3 (c) and (d). The indirect band gap at T point is 0.82 eV at ambient pressure and it reduces to 0.79 and 0.51 eV at 3 GPa and 10 GPa respectively. The band gap at the high symmetry point Y is 0.83, 0.82 and 0.6 eV at 0, 3 and 10 GPa respectively. At 10 GPa significant portions of CBM and VBM crosses the Fermi level and contribute to the DOS. The total DOS shows an indirect band gap 0.058eV, the position of the VBM and CBM are -0.042 and 0.015eV with respect to Fermi level at 0 pressure (figure 2b).

To get information about bulk modulus and its derivative a third-order Birch-Murnaghan equation of state (EOS) was employed to fit the P-V data (figure 5 b and d). The Birch-Murnaghan EOS is expressed as-

$$\mathbf{P(V)} = \frac{\mathbf{3}}{\mathbf{2}}\mathbf{B_0}[(\frac{\mathbf{V_0}}{\mathbf{V}})^{\frac{\mathbf{7}}{\mathbf{3}}} - (\frac{\mathbf{V_0}}{\mathbf{V}})^{\frac{\mathbf{5}}{\mathbf{3}}}] \times \{\mathbf{1} + \frac{\mathbf{3}}{\mathbf{4}}(\mathbf{B_0^{'}} - \mathbf{4})[(\frac{\mathbf{V_0}}{\mathbf{V}})^{\frac{\mathbf{2}}{\mathbf{3}}} - \mathbf{1}]\} \quad \textbf{(1)}$$

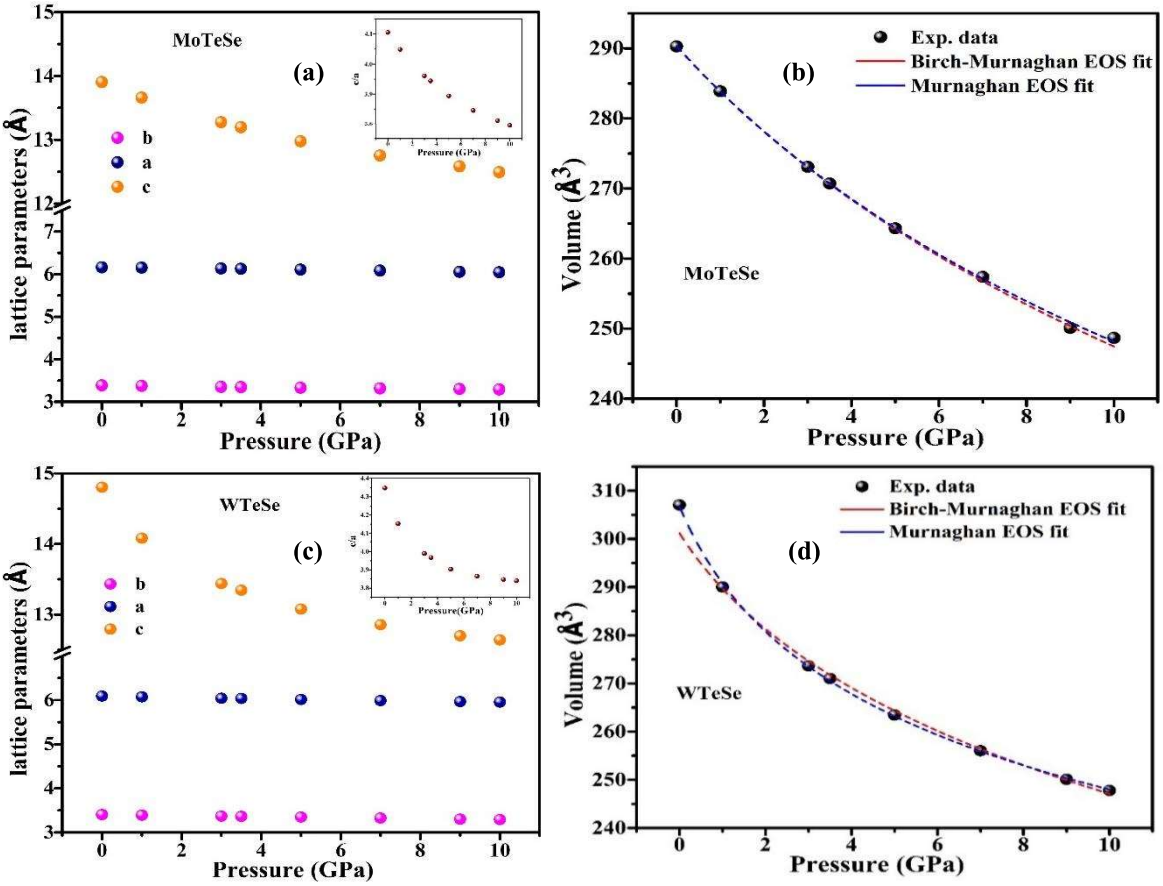

Figure 7.A.5 (a) Evolution of lattice parameters a, b and c with pressure for MoTeSe and (c) WTeSe; (b) Volume as a function of pressure and the fitting of P-V data with 3rd order Birch-Murnaghan and Murnaghan equation of state for MoTeSe and (d) WTeSe.

The fitting (equation 1) yields unit cell volumeV_0=290.33(301.19) Å^3, bulk modulus B_0 =41.79 (21.35) GPa and derivative of bulk modulus B_0' = 5.03(9.58) for MoTeSe (WTeSe). The larger value of B_0' signifies a stronger change in volume compressibility under pressure. Our calculated values are close to $MoTe_2$ and WTe_2 [357], [362] but smaller than $MoSe_2$[205]. The P-V data is also fitted with Murnaghan EOS-

$$\mathbf{P(V) = \frac{B_0}{B_0'}\left[\left(\frac{V_0}{V}\right)^{B_0'} - 1\right]} \quad \textbf{(2)}$$

The extracted values (equation 2) are V_0=290.36 Å^3, B_0=41.72 GPa and B_0'=5.03 for MoTeSe and V_0=306.77 Å^3, B_0=14.34 GPa and B_0'=9.59 for WTeSe.

7.A.4 Conclusions

We have theoretically investigated the electronic band structure and DOS of two compounds MoTeSe and WTeSe at ambient conditions. The present work shows Dirac dispersion without crossing in case of WTeSe. No such dirac dispersion is noticeable in MoTeSe. Again, both the compounds MoTeSe and WTeSe are semimetallic. We Have also explored pressure induced electronic changes up to 10 GPa. The investigation also evinced semimetal to metal transition near 3 GPa in these compounds because of decrease in lattice parameters and increased interaction in interlayer bonds.

B. First-principles calculation of Sb_2Te_3 topological insulator under pressure

7.B.1 Introduction

It is known that A_2B_3(A=Sb/Bi, B=Te/Se) type of materials crystallizes in the rhombohedral structure with space group R-3m (166) under atmospheric conditions. The quintuple layers (QL) are made by 5 atomic layers of B(1)-A-B(2)-A-B(1) and bonded by weak van der Waals bonding. The atomic layers are themselves connected by stronger covalent bonding. These V2-VI3 semiconducting materials are Topological insulators with topologically protected surfaces states within a bulk band gap. These layered materials have taken tremendous recent research interests for room temperature thermoelectric application[201], [218], [368]–[372]. Application of pressure provides another route to study superconductivity[189], [212], [373] in these class of materials. Moreover, high pressure studies on these special class of materials unveil many distinctive phenomena like electronic topological transition(ETT)[195], [244], [247], [248], structural transitions[186], [374] and electronic transitions like semiconductor to metal transition[105]. Pressure can induce changes in atomic distance and electronic properties to produce rich physics. The ETT or Lifshitz transition is associated with Fermi surface reconstruction without breaking of symmetry. The changes in density of states near the Fermi energy occurs when van Hove singularity passes through the Fermi level. Experimentally ETT has been assessed in materials by c/a or Raman width anomaly and resistivity measurements. Theoretically ETT has also been observed by capturing the changes in shape or size of band extrema. Again, the issue of electronic transition like semiconductor to metal transition or a metal insulator transition under pressure provokes considerable research interest in this family of compounds. Experimentally a semiconductor to metal transition was verified by [105], [374] in Bi_2Te_3. However theoretically this observation was missing in the report of [375]. Theoretical finding of a semiconductor to metal transition was assigned in Sb_2Te_3

topological insulator[207]. Experimental realization of this particular transition is yet to be observed in this material. Although metallization [376] was verified by transport measurements in Bi_2Se_3 theoretically [377] it was not obtained in this material. So considerable number of controversies is there with this particular transition and needs further research. In this report we reveal theoretical study of an ETT along with metallization in Sb_2Te_3. We also explore detail analysis behind this transition.

7.B.2 Methods

We performed DFT calculations using Vienna ab initio simulation package (VASP) [378] with a projector-augmented-wave (PAW) method. We adopted local-density approximations (LDA) and generalized gradient approximation (GGA) as exchange-correlation proposed by Perdew-Burke-Ernzerhof (PBE). All atoms of Sb_2Te_3 were fully relaxed with conjugate-gradient algorithm until a force is less than 0.01eV $Å^{-1}$ and the energy convergence criteria was put to 10^{-6} eV. The electronic calculations were performed using Γ-centred K-mesh of 12×12×1 with a plane-wave energy cutoff of 400eV, spin orbit coupling (SOC) was included in the calculations. For the DOS calculation we used NEDOS=1000 and NBANDS=100.

7.B.3 Results and Discussions

Sb_2Te_3 crystallizes in rhombohedral R-3m space group (S.G =166) structure with five atoms per unit cell. One quintuple layer (QL) contains five alternative sheets [Te1-Sb-Te2-Sb-Te1] of Sb and Te atoms Figure 7.B.1 (a). High-pressure studies are very helpful to realize material properties and it opens up new opportunities by reducing the interatomic distances with increasing pressure. Application of external pressure allows various electronic and structural deformations.

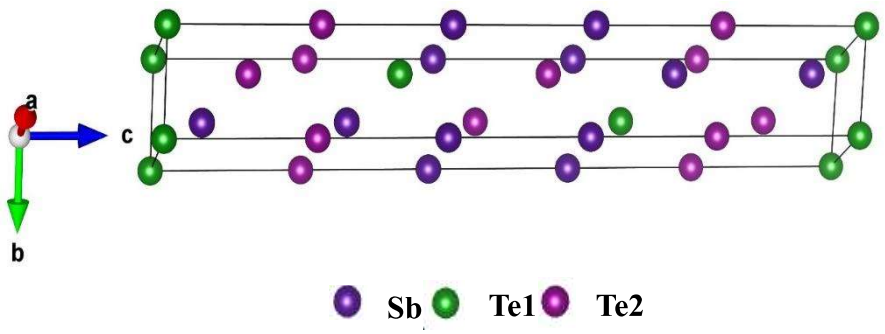

Figure 7.B.1 Crystal structure of Sb_2Te_3.

The optimized lattice parameters are taken as a=b=4.322Å, c= 30.867 Å [207] for the theoretical calculation of Sb_2Te_3 at ambient pressure. The Sb atoms occupies the 6c (0, 0, 0.3977) while the Te atom resides at 6c (0, 0, 0.2132) and 3a (0,0,0) wychoff sites. We have used LDA and GGA-PBE approximation for evaluation of the electronic transition. GGA predicts usual insulating bulk character of this material, inclusion of SOC increases the band gap (0.18 eV) of the system shown in Figure 7.B.3 (a). The conduction band minimum is along Γ-point and the valence band maxima is along Z-F symmetry line. The DOS in Figure 7.B.3 (c) demonstrate p-type behavior which is in line with the previous experimental results [379]. In Figure 7.B.3 (d) The density of states showing finite bandgap (0.22 eV) between CBM and VBM indicating insulating character by GGA approximation. The obtained result with LDA approximation indicates a metallic transition at 2 GPa. The conduction bands are crossing the Fermi level at gamma symmetric point, it is shown in Figure 7.B.2 (a). The CBM and VBM meets at Γ-point, with addition of SOC it becomes an indirect band gap semiconductor with 0.19 eV gap Figure 7.B.2 (b). Although both the approximation (GGA, LDA) underestimates the van der Waals weak interaction both results are showing different characteristics. Inclusion of SOC in LDA method opens up a gap. The occupancy of valence band maxima and conduction band minima is also inverted.

Previously we have seen, the local density approximation (LDA) underate the lattice parameters and volume compared to experimental values, whereas GGA-PBE tend to overestimate the lattice parameters [380]. Previous reports in DFT calculations also revealed that the LDA notably underrated phase-transition pressures for various metallic and covalent systems, while the GGA shows a compliance with experiment [381]. GGA approximation rely on the local density as well as on the spatial variation of the density. Again, at ambient pressure the density of states near Fermi energy is mainly contributed by Sb atoms for conduction band. It is Te atoms which notably participate in valence band near the Fermi level. The band structure and DOS using GGA-PBE approximation has been shown at Figure 7.B.2. The band structure has a finite bandgap at both ambient and higher pressures. No band crossing is visible in 2 GPa Figure 7.B.3(b). For both Figure 7.B.3(c) and (d), Sb atoms has relatively larger participation in conduction band whereas for valence bands, Te takes dominant role.

Again, when a band extremum corresponded with Van Hove singularity crosses the Fermi level, we observe an ETT. As a result, the redistribution of DOS occurs which ultimately creates a second-order isostructural phase transition. In this process no variation in Wyckoff positions and no volume discontinuity is observed. Hence this results in a modification of the elastic constants and change of the compressibility of the systems. The band structure obtained at 7 GPa Figure 7.B.4(a) manifests changes in band shapes. The band gap decreases at Γ-point whereas it is increased near Z point compared to ambient condition. This is also observed in previous reports on topological insulator systems[189]. The changes in shape and positions of the CB and VBs are associated with ETT. We have shown comparative study of ETT with their ambient structure.

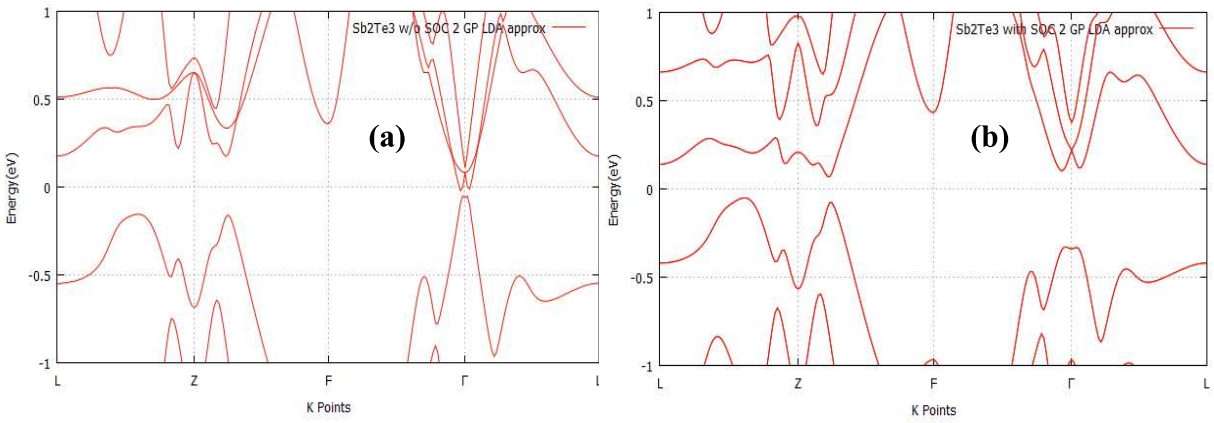

Figure 7.B.2 Bandstructure of Sb_2Te_3 taking LDA approximation (a) without SOC; (b) with SOC.

To get information about bulk modulus and its derivative a third-order Birch-Murnaghan equation of state (EOS) was employed to fit the P-V data Figure 7.B.5(a). The Birch-Murnaghan EOS is expressed as-

$$\mathbf{P(V) = \frac{3}{2} B_0 [(\frac{V_0}{V})^{\frac{7}{3}} - (\frac{V_0}{V})^{\frac{5}{3}}] \times \{1 + \frac{3}{4}(B_0' - 4)[(\frac{V_0}{V})^{\frac{2}{3}} - 1]\}} \qquad \textbf{(7.B.1)}$$

The fitting (equation 1) yields unit cell volumeV_0=166.9154 $Å^3$, bulk modulus B_0 =38.8401 GPa and derivative of bulk modulus B_0' = 3.6472 for Sb_2Te_3. The larger value of B_0' signifies a stronger change in volume compressibility under pressure. We have also fitted our P-V data with Murnaghan EOS-

$$\mathbf{P(V) = \frac{B_0}{B_0'} [(\frac{V_0}{V})^{B_0'} - 1]} \qquad \textbf{(7.B.2)}$$

The obtained values from equation 2 remain same as fitted by B-M EOS. Our B_0 and B_0' values are close to the value reported in [385], [386].

The rate of decrease of the lattice parameter c with pressure is relatively larger than a or b because of the natural tendency of forming layered structure Figure 7.B.4(b). The ratio of

c/a parameter has also been described in Figure 7.B.5(b). The minimum in c/a ratio represents presence of an ETT in between 4-6 GPa.

Table 7.B.1 Comparisons of ETT pressure in different TI materials.

Materials	Ambient Structure	**ETT (GPa)**
Sb_2Te_3	R-3m	3.2[193]; 3.5[244]
Sb_2Se_3	Pbnm	2.5 [382]
Sb_2S_3	Pnma	5 [194]
Bi_2Te_3	R-3m	3[192]; 4 [376]
Bi_2Se_3	R-3m	3 [383]
Bi_2S_3	Pnma	4–6 [384]
Sb_2Te_3	R-3m	4-6 [**This work**]

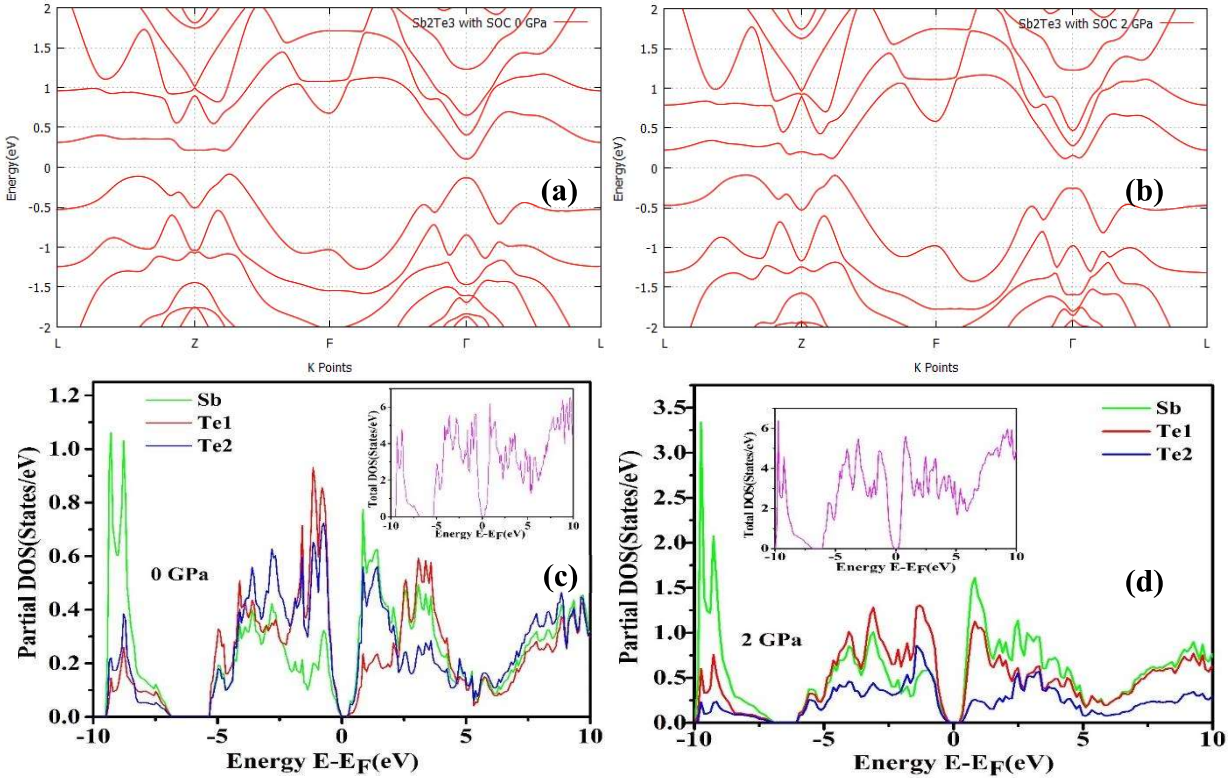

Figure 7.B.3 Bandstructure of Sb_2Te_3 taking GGA approximation (a) at ambient pressure; (b) at 2GPa; (c) Partial and total DOS of Sb_2Te_3 at ambient pressure; (d) at 2 GPa.

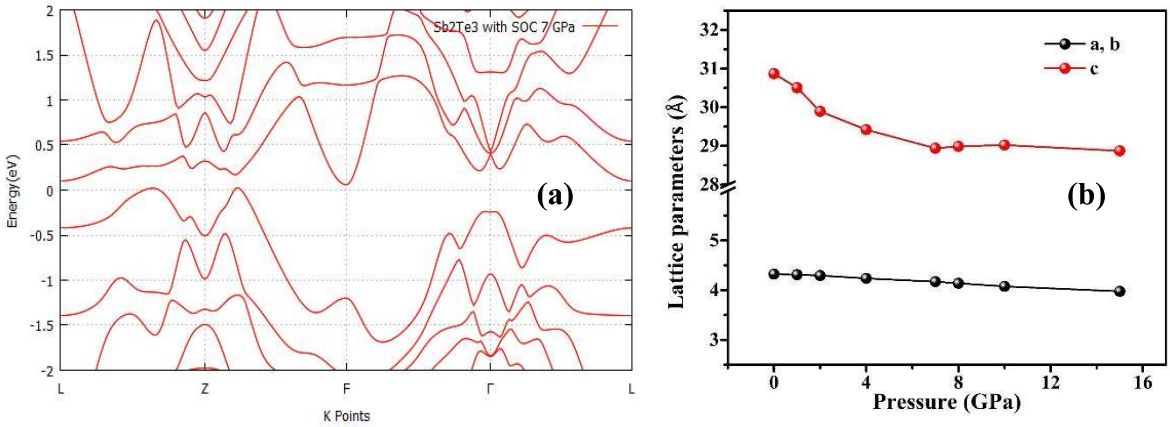

Figure 7.B.4 Bandstructure of Sb_2Te_3 taking GGA approximation (a) at 7GPa pressure; (b) Comparison of lattice parameters with pressure.

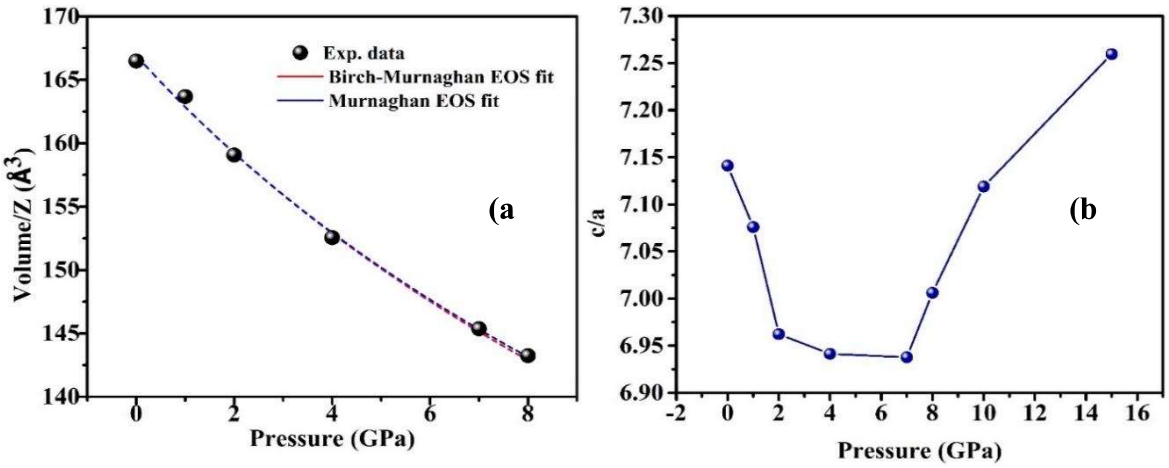

Figure 7.B.5 (a) Volume as a function of pressure and the fitting of P-V data with 3rd order Birch-Murnaghan and Murnaghan equation of state for Sb_2Te_3; (b) c/a ratio as a function of pressure.

The electronic topological transition was explained by decrease in bond length and electron transfer from Sb to Te atom and increase in charge density[207]. We also investigated the surface state under pressure. The band structure evinced a Dirac point (highlighted with a blue circle) centered at the Γ-point with linear dispersion for the ambient phase, however the band crossings remain intact even at higher pressure. This further denotes that the non-trivial surface state is protected even in extreme conditions. The only difference is that the bulk band gap is reduced at 7 GPa compared to zero pressure. The surface state electronic

structures are displayed in Fig. 6(a) and (b). Our calculation consistent with strain induced topological insulating phase As_2Te_3[387].

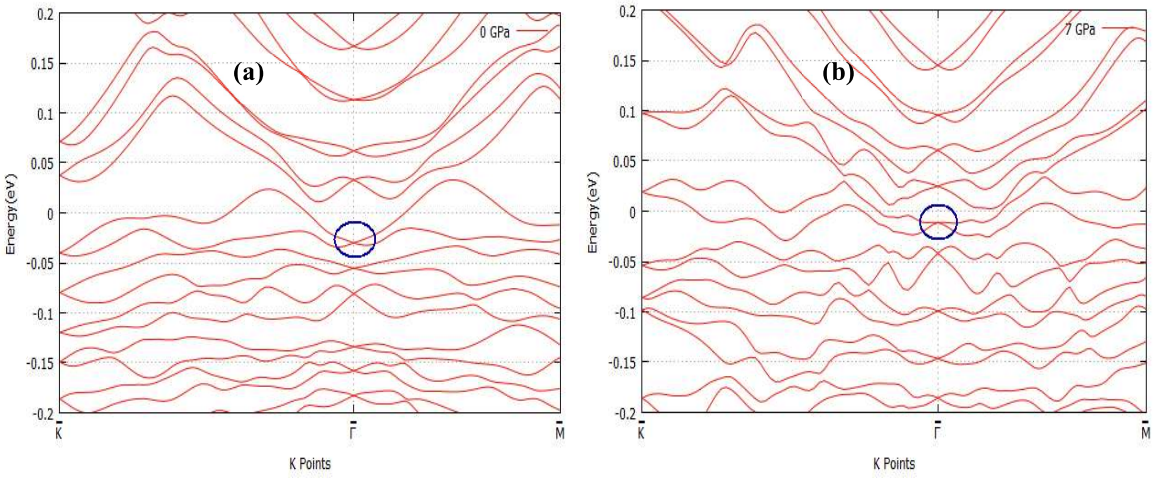

Figure 7.B.6 Electronic structure of the surface of Sb_2Te_3 along its (111) surface at (a) 0 pressure and (b) 7 GPa. The electronic states forming the Dirac cone have been marked with blue circle.

7.B.4 Conclusions

We observed an ETT together with an additional electronic transition in Sb_2Te_3 from the theoretical calculations. The former is due to Fermi surface redistribution whereas the later occurs because of the closure of bulk band gap and inversion of band extrema. The semiconductor to metal transition is however absent in GGA approximation.